International Journal of Biochemistry and Cell Biology 108 (2019) 98–110

Contents lists available at ScienceDirect

International Journal of Biochemistry and Cell Biology

journal homepage: www.elsevier.com/locate/biocel

Induction of phosphatase shatterproof 2 by evodiamine suppresses the proliferation and invasion of human cholangiocarcinoma

Biqiang Zhu[a,b], Lei Zhao[a], Yang Liu[a], Ye Jin[a], Jing Feng[a], Fuya Zhao[a], Jiayu Sun[a], Rui Geng[a], Yunwei Wei[a,*]

[a] Department of Oncological and Endoscopic Surgery, The First Affiliated Hospital of Harbin Medical University, No. 23 You Zheng Street, Harbin 150001, Heilongjiang, China

[b] Translational Medicine Research and Cooperation Center of Northern China, Harbin 150081, Heilongjiang, China

ARTICLE INFO

Keywords:
Evodiamine
Apoptosis
interleukin-6
Epithelial-to-mesenchymal transition
Signal transducer and activator of transcription 3
Phosphatase shatterproof 2

ABSTRACT

Cholangiocarcinoma (CCA) is one of the most common fatal carcinomas and is well known to be lack of effective treatment. Thus, novel therapeutic strategies are greatly needed. Evodiamine, a quinozole alkaloid isolated from evodia rutaecarpa Bentham, has been demonstrated to exhibit anti-tumor effects on many cancer cells. However, little is known in terms of the effects on cholangiocarcinoma. In this study, we studied whether this traditional Chinese Medicine could serve as new potential therapeutic drugs to treat CCA. We discovered that evodiamine inhibited CCA cell proliferation and induced apoptosis. Moreover, evodiamine inhibited CCA cell migration and invasion. Mechanistically, our studies demonstrated that evodiamine inhibited the activation of IL-6 -induced STAT3 signaling activation, and the inhibitory effect was likely due to the upregulation of phosphatase shatterproof 2 (SHP-2), a negative feedback regulator of IL-6/STAT3. Blockage of SHP-2 through small interference RNA (siRNA) abolished the evodiamine -induced IL-6/STAT3 signaling inhibition. Moreover, in vivo experiment showed evodiamine inhibited the tumor growth of nude mice bearing TFK-1 xenografts. In summary, our results implied evodiamine as a promising anti-cancer agent in the treatment of CCA, and the mechanism is likely due to the inhibition of IL-6/STAT3 signaling with upregulating the expression levels of SHP-2.

1. Introduction

In recent years, cholangiocarcinoma (CCA) becomes the second most common primary hepatic malignancy in South America and Asia (Rizvi and Gores, 2017). Surgical resection is the only potentially curative treatment. However, the resectability rate remains low (Razumilava et al., 2011; Rizvi et al., 2014). In addition, complete surgical resection is often followed by local recurrence or metastasis, and the 5-year survival rate was only 5–10% (Khuntikeo et al., 2014; Zhimin et al., 2013). Therefore, novel strategies are urgently needed.

Signal transducer and activator of transcription 3 (STAT3) belongs to the STAT family, is initiated and regulated by interleukin-6 (IL-6) family cytokine receptor-associated Janus kinase (JAKs), which integrates signals from extracellular stimuli and regulates the transcription of target genes (Vogt and Hart, 2011), participating in oncogenesis, such as apoptosis inhibitors (Bcl-2, and Survivin), cell-cycle regulators (cyclin D1) and EMT regulators (MMPs, vimentin) (Burdon et al., 2002; Qin et al., 2012; Xiang et al., 2016). Recently, many studies have reported that STAT3 plays an important role in metastasis and that its expression is negatively correlated with surgical outcome in CCA (Roy et al., 2017; Tong et al., 2017; Yao et al., 2016). Tanjak et al.(2018) discovered a significant increase in serum IL-6 concentrations in CCA patients compared with controls, as well as an elevated positive correlation between IL-6 and the size of the tumor (Mott and Gores, 2007). Thus, STAT3 signaling is considered a potential therapeutic target in CCA (Bartolowits et al., 2017; Shi et al., 2017b).

Many anti-tumor strategies have been performed via STAT3 singling pathway inhibition, such as AZD1480 (Xin et al., 2011), S31-201 (Siddiquee et al., 2007), peptides (Chin et al., 2017; Ma et al., 2014), specific small interfering RNAs (Liu et al., 2017b) and natural products (Jin et al., 2017). Recently, we screened evodiamine, a quinozole alkaloid isolated from the dried, unripe fruit of evodia rutaecarpa Bentham as a potent and specific STAT3 pathway inhibitor. Previous studies showed evodiamine has effects on cardiovascular diseases, nervous system diseases, hepatitis and diabetes (Jiang et al., 2017; Wang et al., 2013; Wu et al., 2017a; Zhu et al., 2016). Recently, increasing attention has focused on the anti-cancer effects of evodiamine including hepatocellular carcinoma (HCC), glioblastoma, human urothelial cell

* Corresponding author.
E-mail address: hydwyw11@hotmail.com (Y. Wei).

https://doi.org/10.1016/j.biocel.2019.01.012
Received 17 September 2018; Received in revised form 23 December 2018; Accepted 21 January 2019
Available online 22 January 2019
1357-2725/

carcinoma, breast cancer, prostate cancer and lung cancer (Fang et al., 2014; Hu et al., 2017a; Kan et al., 2007; Shi et al., 2017a; Wang et al., 2014; Wu et al., 2017b). Importantly, evodiamine have been shown to exhibit anti-tumor effects via mediating STAT3 signaling pathway (Yang et al., 2013; Zhao et al., 2015a). Thus, we performed experiments to find whether evodiamine can be used as a new STAT3 inhibitor exhibiting potential effects on CCA.

In this study, we investigated the effects of evodiamine on CCA cell growth, apoptosis and metastasis *in vitro* and *in vivo* and the molecular mechanisms responsible for these effects. We report for the first time that evodiamine induces cell death and suppresses metastasis by influencing IL-6/STAT3-mediated signaling in CCA, and further study demonstrated this blockage was mediated by a negative feedback regulator, SHP-2. In conclusion, we provide experimental evidence for the potential application of evodiamine as a novel, natural, anti-tumor treatment for CCA through blocking IL-6-induced STAT3 signaling.

2. Materials and methods

2.1. Cells and culture

Two human CCA cell lines were used, HuCCT-1 and TFK-1. Cells were incubated in RPMI 1640 medium containing 10% fetal bovine serum (BI) supplemented with 1% penicillin-streptomycin solution (Gibco) at 37 °C in a humidified atmosphere of 5% CO_2.

2.2. Chemicals and reagents

Evodiamine (purity > 99%) was purchased from Sellevk Chemicals (USA) and dissolved in dimethyl sulfoxide (DMSO) at 100 mmol/L. The final concentration of DMSO in the culture medium was maintained at 0.1%, which showed no cytotoxicity to the CCA cells. Sodium pervanadate and recombinant human IL-6 were purchased from Sigma-Aldrich (St. Louis, MO, USA).

2.3. Cell viability assay

Cells in the logarithmic phase of growth were collected, and 2000 cells were seeded into each well of a 96-well plate and cultured for 24 h in the medium described above. The indicated concentrations of evodiamine were added and incubated with the cells for 24, 48 or 72 h. Finally, cell viability was measured by CCK-8 assay, according to the manufacturer's instructions (Dojindo, Japan).

2.4. Colony formation assay

700 cells per 35-mm dish were plated before being treated. Then, 1 ml of medium with indicated concentrations of evodiamine was added to each dish. After 14 days, the cells were fixed using 70% ethanol and stained using crystal violet (Sigma, USA). Colonies, defined as a minimum of 50 cells in a group, were counted.

2.5. Hoechst 33258 staining

TFK-1 cells were placed at a final concentration of 5 × 105 cells per well in a six-well plate, which was pretreated with 0, 20, or 40 μM evodiamine for 24 h. The cells were subsequently fixed, washed three times with phosphate buffered saline (PBS), and stained with Hoechst 33258 (Sigma-Aldrich) according to the manufacturer's protocol. Apoptotic features were assessed by analyzing chromatin condensation and by staining the fragments under an inverted fluorescent microscope (Olympus, Center Valley, PA, United States).

2.6. Apoptosis assay

Cells (2×10^5/well) in 6-well plates were treated with the indicated drug concentrations for 24 h and were then collected and washed twice in ice-cold PBS. Apoptosis was assessed using an Annexin V-FITC kit (BD Pharmingen, USA), according to the manufacturer's instructions, with a BD Accuri™ C6 flow cytometer (Becton-Dickinson, USA).

2.7. Wound-healing assay

TFK-1 cells were seeded into 6-well plates and scraped with the end of 200ul pipette tips. After the plates were washed with PBS to remove detached cells, the remaining cells were then incubated in complete growth medium containing 0, 2, 4 or 8 μM evodiamine solution for 24 h. Cell migration was observed under a phase-contrast microscope at 40× magnification after 0 and 24 h. TFK-1 cells that had migrated into the scraped area in six random fields of view were quantified by computer-assisted microscopy.

2.8. Transwell migration assay

Transwell membranes were pre-coated with 50 μl of a 1:1 mixture of Matrigel and RPMI medium. TFK-1 cells were treated with 0, 4 or 8 μM evodiamine for 24 h and then harvested. Subsequently, RPMI with 10% FBS was added to the bottom chamber, and cells treated as indicated were allowed to incubate for 48 h. Cells that migrated to the bottoms of the filters were stained with 0.1% crystal violet. Finally, six random fields of view of each transwell membrane were analyzed and averaged.

2.9. Immunofluorescence assay

TFK-1 cells were seeded into confocal dishes (1×10^4/well). We fixed the cells in 4% paraformaldehyde and incubated in 10% goat serum and 1% Triton to increase cell membrane permeability after the morphology had returned to normal. We then incubated the cells with rabbit anti-human anti-p-STAT3 (Tyr705) antibody overnight at 4 °C, followed by incubation with a red fluorescence-labeled goat anti-rabbit secondary antibody for 30 min in the dark. Finally, nucleus was stained using DAPI for 15 min in the dark, and the green and blue fluorescence intensities were observed by fluorescence microscopy. Each immunofluorescence assay was repeated 3 times.

2.10. siRNA and plasmid transfection

For RNA interference, siRNA negative control (NC) and SHP-2 siRNA were purchased from GenePharma (Suzhou, Zhejiang, China), The sequences targeting SHP-2 were as follows: 5′- GGAGAACGGUUU GAUUCUUTT-3′ (siRNA-1) and 5′- AAGAAUCAAACCGUUCUCCTC-3′ (siRNA -2). For plasmid overexpression, STAT3C was obtained from Liaoning Baihao Biological Technology Co. Ltd. (Shen yang, Liaoning, China). These plasmids or siRNAs were subsequently transfected into cells using Lipofectamine 2000 reagent (Invitrogen, CA).

2.11. Nucleus protein isolation and western blot

We extracted nucleus protein according to the manufacturer's instructions via a nucleus and cytoplasmic protein extraction kit (Beyotime). Aliquots containing 30 μg of lysed protein were separated by 10% SDS-PAGE, and the proteins were then transferred onto PVDF membranes (Millipore, USA). After blocking, the membranes were incubated with specific primary and secondary antibodies. The targeted protein band was visualized via enhanced chemiluminescence. The intensity was measured using ImageJ software after normalization to the corresponding loading control. Primary antibodies were used: cleaved caspase 3, cleaved caspase 9, Bcl-2, Bax, E-cadherin, vimentin, MMP-2, MMP-9, p-STAT3 (Tyr705), p-STAT3 (Ser727), STAT3, SHP-1, SHP-2, TC-PTP, Histone H3 and β-actin (Cell Signaling Technology).

2.12. Animal studies

Exponentially growing TFK-1 cells were suspended in serum-free culture medium (at a density of 1×10^7 cells in 0.2 mL) and injected subcutaneously into the right axilla of recipient mice. After 1 week of implantation, tumor-bearing mice were randomly divided into two groups (control and 20 mg/kg), with six animals in each group. Evodiamine was administered to the mice in the treatment group by intraperitoneal injection every 2 days at 20 mg/kg. Control animals received intraperitoneal injections of vehicle (10% DMSO and 90% PBS). Tumor volume was measured using calipers and estimated according to the following formula: tumor volume (mm^3) $(L \times W^2)/2$, where L and W represent the length and width of the tumor, respectively. After 4 weeks of treatment, all mice were killed, and tumor tissue were generated for further analysis.

2.13. Immunohistochemistry

Formalin-fixed, paraffin-embedded sections (4 μM) were deparaffinized in xylene, rehydrated in graded alcohol, and rinsed in phosphate-buffered saline (PBS). Endogenous peroxidase activity was blocked with 3% hydrogen peroxide in methanol for 20 min. Epitope retrieval was performed in citrate buffer for 5 min at 100 °C. Slides were incubated with mouse primary antibodies at 4 °C overnight. After washing three times with fresh PBS, the sections were subsequently incubated with secondary antibody at room temperature for 30 min. For visualization of the reaction, the diaminobenzidine-tetrahydrochloride was stained, then counterstained with hematoxylin, dehydrated and cover slipped. Two observers without knowledge of the studies' data performed evaluation of the staining.

2.14. Statistical analysis

All data were expressed as mean ± SD of three independent experiments. Statistical significance was determined using Student's *t*-test or ANOVA. A *P* value of less than 0.05 was considered statistically significant. Detailed description of Methods can be found in the online Supporting Information.

3. Results

3.1. Evodiamine inhibits CCA cell proliferation

The chemical structure of evodiamine is shown in Fig. 1A (Fang et al., 2014). To explore the effect of evodiamine on the growth of CCA cells, two CCA cell lines, HuCCT-1 and TFK-1, were treated with evodiamine at different concentrations (0, 5, 10, 20 or 40 μM) for different time periods (24, 48 or 72 h), and analyzed by CCK 8 assay. The results showed that the viability of HuCCT-1 and TFK-1 cells was inhibited by evodiamine in a time- and dose-dependent manner (Fig. 1B and C). To determine the long-term growth inhibitory effect of evodiamine, we pre-incubated HuCCT-1 and TFK-1 cells with evodiamine (0, 20 or 40 μM) for 24 h, washed the cells, and cultured them for 14 additional days in complete growth medium. As shown in Fig. 1D and E, CCA cell colony formation was significantly reduced by evodiamine in a dose-dependent manner. These results suggest that evodiamine inhibits the proliferation of CCA cells.

3.2. Evodiamine induces apoptosis in human CCA cells

To determine if the inhibitory effect of evodiamine on CCA cells was associated with apoptosis, TFK cells were stained with Ho-chest33258 and observed under a fluorescence microscope (Fig. 2A). After being treated with 0, 20 or 40 μM evodiamine for 24 h, nuclear chromatin condensation and fragmented punctuate blue nuclear fluorescence were observed in TFK-1 cells, while the control cells were normal and intact nuclei. The result suggested that evodiamine might induce CCA cancer cell apoptosis.

To further verified the pro-apoptosis effect of evodiamine, TFK-1 cells were exposed to the indicated concentrations of evodiamine (0, 20 and 40 μM) for 24 h followed by flow cytometry. As the data showed, evodiamine significantly increased apoptotic cell populations, and decreased the viable cell population compared to the vehicle control group, in a dose- dependent manner (Fig. 2B). In addition, the activation of caspase 3 and caspase 9, key molecules of the apoptosis pathway (Galluzzi et al., 2016), was evaluated by western blot. As expected, evodiamine induced the cleavage of caspase 3 and caspase 9 in a dose-dependent manner (Fig. 2C). Furthermore, we examined the protein expression levels of apoptosis-related genes, including B-cell lymphoma 2 (Bcl-2) and Bcl-2-associated X protein (Bax) (Reyna et al., 2017). After 24 h of treatment with evodiamine, a significant reduction in Bcl-2 expression was observed, while Bax levels were significantly increased in a dose-dependent manner (Fig. 2D). Taken together, these results suggest that the effect of evodiamine on CCA cell viability is at least partially mediated via apoptosis.

3.3. Evodiamine suppresses CCA cell migration and invasion

To explore the anti-metastasis potential of evodiamine, we first examined the ability of evodiamine to modify cell invasion and migration by the Matrigel-based invasion assays and wound-healing assays in a low concentration (0, 4 or 8 μM), not induce cell apoptosis. The results showed that evodiamine significantly inhibited CCA cell invasion in a dose-dependent manner through Matrigel membrane (Fig. 3A and C). Additionally, evodiamine dose-dependently decreased the migration of TFK-1 cells in the wound-healing assay (Fig. 3B and C). Both the wound-healing and Matrigel-based invasion assays suggested that evodiamine could inhibit the motility of CCA cells.

Epithelial-to-mesenchymal transition (EMT) is known to be a critical event in tumor invasion and migration (Thiery et al., 2009). We found the 24 h treatment of TFK-1 cells with 0, or 10 μM evodiamine changed CCA cell morphology from fibroblast-like mesenchymal phenotype to round, epithelioid phenotype. (Fig. 3D). To further assessed the results, the protein levels of matrix metalloproteinase-9 (MMP-9), matrix metalloproteinase-2 (MMP-2) and vimentin, which are typical EMT markers (Torzilli et al., 2012), were significantly reduced after the treatment of evodiamine, whereas expression levels of the epithelial marker E-cadherin was greater in the evodiamine-treated group than in the control group (Fig. 3E). Accordingly, the anti-metastasis activity of evodiamine observed in the wound-healing and Matrigel-based invasion assays might be at least partially due to reversing the EMT change of CCA cells.

3.4. Inhibitory effects of evodiamine on CCA cell proliferation and metastasis are dependent on the suppression of IL-6/STAT3 activation

The results presented above suggest that evodiamine is a wide-spectrum inhibitor of tumor cells on various aspects of cell biology: suppressing cell proliferation, migration and invasion, and promoting apoptotic cell death. While these effects together might account for the anti-CCA efficacy of evodiamine, we intended to further decipher the underlying molecular and signaling mechanisms. To this end, we conducted the following experiments.

First, we investigated the potential involvement of STAT3 that are known to be critical to the growth and metastasis of CCA cells. TFK-1 cells were treated with various concentrations of evodiamine (0, 5, 10, 20 or 40 μM) for 24 h or treated with 20 μM evodiamine for various times (0, 1, 2, 4 or 8 h). Our data demonstrated that evodiamine significantly decreased the phosphorylated /activated form of STAT3 (Tyr705; p-STAT3) in dose-dependent manner and time-dependent manner, whereas the total STAT3 protein expression was unchanged (Fig. 4A and B). In addition, we tested another phosphorylation site of

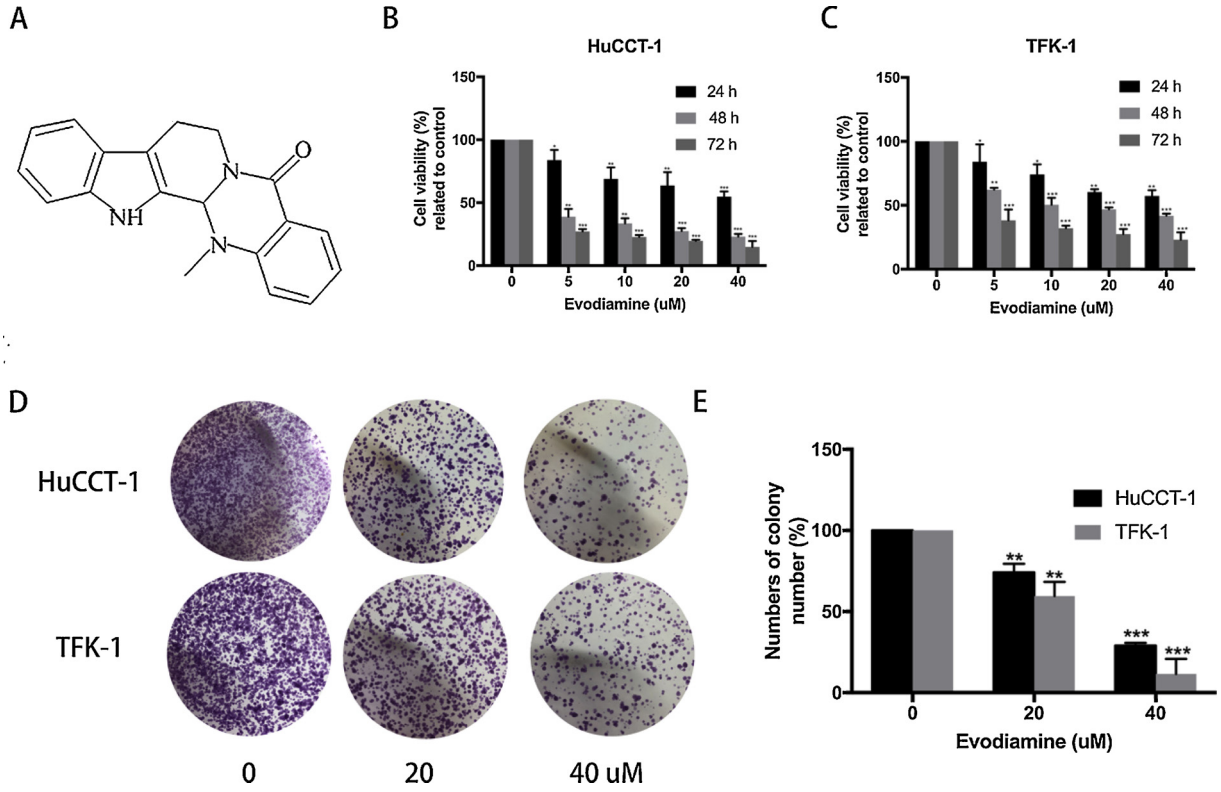

Fig. 1. Evodiamine inhibits CCA cell proliferation.
The inhibitory effects of evodiamine on the survival of HuCCT1 and TFK-1 cells. (A) Chemical structure of evodiamine. (B & C) Cell viability of HuCCT-1 and TFK-1 was assessed by CCK8 assay and presented as percent of control. (D & E) The anti-proliferative effect of evodiamine on CCA cells was assessed by colony formation assay. The data are expressed as the mean SD of 3 replicate experiments. Significant differences from the control are indicated by $*P < 0.05$, $**P < 0.01$, $***P < 0.001$.

STAT3 at Ser727. However, data showed that there was no significant change. Second, to examine whether evodiamine suppressed STAT3 activation by inhibiting the upstream signaling component IL-6 (interleukin-6) that normally induces STAT3 phosphorylation in CCA cells, we pretreated the CCA cells with evodiamine (20 μM) for 24 h followed by stimulation with various concentrations of IL-6 (0, 10 or 20 ng/ml) for 15 min. As shown in Fig. 4C, the IL-6 induced-STAT3 phosphorylation in a does dependent manners, and was reduced by evodiamine. Consistently, immunofluorescence assay also exhibited a significant decrease in p-STAT3 by evodiamine (Fig. 4D). Moreover, Western blot data further unraveled that the level of nucleic STAT3 was reduced by evodiamine, leaving total STAT3 unaltered (Fig. 4E). These data indicated that evodiamine prevents the translocation of STAT3 from the cytoplasm to the nuclei through suppressing its phosphorylation.

In order to further verify the role of STAT3 in mediating the cellular effects of evodiamine, we transfected the TFK-1 cells with a STAT3C plasmid or an empty vector as a negative control, which is constitutively activated but not tyrosine phosphorylated (Sakaguchi et al., 2012; Weissenberger et al., 2010). Following transfection, the cells were treated with evodiamine at various concentrations for 24 h, and the CCK-8 assay was performed to measure cell growth. Our results showed that the growth of TFK-1 cells was inhibited by evodiamine in a dose-dependent manner, which was partially reversed by STAT3C overexpression (Fig. 4F), indicating that the inhibitory effect of evodiamine on CCA cell growth is dependent on the suppression of p-STAT3. As expected, the levels of cleaved caspase 3 and cleaved caspase 9 were decreased, whereas those of MMP-2 and MMP-9 were increased after STAT3C overexpression (Fig. 4G). p-STAT3 is a key upstream regulator that influences the expression levels of downstream proteins, which plays important roles in STAT3-mediated apoptosis and EMT (Rokavec et al., 2014). In addition, western blot was also performed to show that evodiamine-induced apoptosis and EMT related proteins changes were partially reversed by STAT3C overexpression (Fig. 4H). Accordingly, these results indicated CCA cells inhibition by evodiamine likely through IL-6/STAT3 pathway.

3.5. Inhibitory effect of evodiamine on p-STAT3 (Try705) is mediated by SHP-2

It has been reported that Numerous protein tyrosine phosphatase (PTPs) are negative regulatory factors of STAT3 Tyr705 phosphorylation. Thus, we wondered whether evodiamine-induced inhibition of STAT3 could be due to activation of PTPs. TFK-1 cells were treated with PTP inhibitor sodium pervanadate at different concentrations for 1 h, and with additional 20 μM evodiamine for 2 h. As shown in Fig. 5A, sodium pervanadate reversed the evodiamine-induced suppression of STAT3 activation in a dose-dependent manner. This result suggests that PTPs are involved in the inhibition of STAT3 Tyr705 phosphorylation by evodiamine. To identify which PTP is mediated by evodiamine, the expression levels of SHP-1, TC-PTP and SHP-2 protein was analyzed in TFK-1 cells. However, there were no obvious changes in the expression levels of SHP-1 and TC-PTP (Fig. 5B), but treatment with evodiamine led to increased expression levels of SHP-2 at the protein level (Fig. 5B). In addition, immunofluorescence assay also conformed the increased protein expression in SHP-2 by evodiamine (Fig. 5C). To validate the role of SHP-2 in suppressing the STAT3 signaling, we next explored the influence of gene silencing. TFK-1 cells were transfected with SHP-2 or NC siRNA for 48 h and then treated with 20 μM evodiamine for 2 h. As shown in Fig. 5D, knockdown of SHP-2 by small interfering RNA dramatically reversed the effect of evodiamine on STAT3 phosphorylation at Tyr705. In addition, TFK-1 cells were transfected with SHP-2 or NC siRNA for 48 h and then treated with 20 μM evodiamine for another

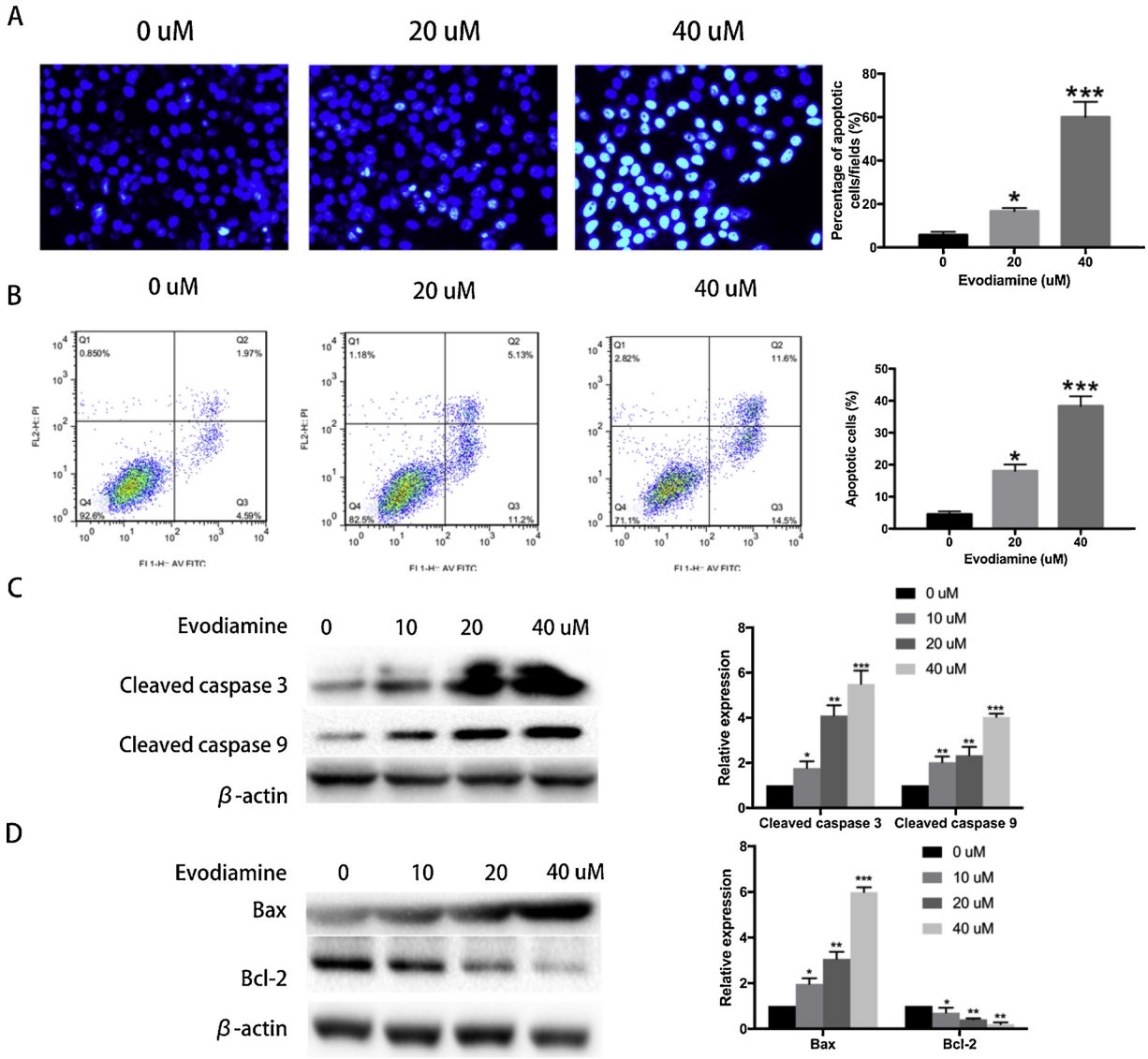

Fig. 2. Evodiamine induced apoptosis in CCA cells.
The pro-apoptosis effects of evodiamine on TFK-1 cells (A) Apoptosis was assessed using Hoechst 33258, and apoptotic features were assessed by observing chromatin condensation and fragment staining (original magnification, × 200) (B) Detection of apoptosis via Annexin V/PI staining (X-axis: annexin V; Y-axis: PI) and analyzed by flow cytometry. (C & D) The protein levels of cleaved-caspase-3, cleaved-caspase-9, Bcl-2 and Bax were measured by Western blot. β-actin served as the loading control. The data are expressed as the mean SD of 3 replicate experiments. Significant differences from the control are indicated by $*P < 0.05$, $**P < 0.01$, $***P < 0.001$.

24 h followed by western blot analysis. Fig. 5E showed evodiamine-induced cell apoptosis and EMT changes were reverted by knockdown of SHP-2. Our results demonstrated that the increase in SHP-2 expression induced by evodiamine may be associated with the down-regulation of constitutive STAT3 activation.

3.6. *Evodiamine inhibits tumor growth in vivo in xenograft tumor-bearing nude mice*

To explore the effects of evodiamine on tumor growth *in vivo*, TFK-1 CCA xenografts were established and grew to a size of 112 mm3, after which evodiamine was given i.p. every 2 days for 4 weeks. We then examined the ability of evodiamine to suppress tumor growth *in vivo*. In general, tumors in the control group grew continuously during the experimental period, whereas tumor growth was significantly suppressed in the evodiamine group (Fig. 6A). The average weight of tumors in the evodiamine-treated animals was 0.99 g, whereas that of tumors in the control animals was 0.18 g (Fig. 6B). The volume changes over the experimental period are provided in Fig. 6C. To evaluate whether evodiamine administration affects normal physiology, we treated non-tumor-bearing mice at the same dose of every 2 days at 20 mg/kg for 4 weeks. No apparent toxicity-related events or significant body weight changes were observed in the evodiamine-treated animals (Fig. 6D). To understand the effects of evodiamine on CCA *in vivo*, we then measured the expression levels of SHP-2, p-STAT3 (Tyr705), cleaved caspase 9 and vimentin. The results revealed that evodiamine treatment reduced the expression levels of p-STAT3 (Tyr705) and vimentin and increased that of cleaved caspase 9 and SHP-2 (Fig. 6E). Immunohistochemistry was performed in xenograft tissue. Results showed that evodiamine effectively suppressed the expression levels of proliferation marker (Ki- 67), metastasis related molecules (vimentin) and p-STAT3, whereas induced the expression levels of apoptotic marker (cleaved caspase 3) and SHP-2 in tumor tissues (Fig. 7A&B). Together, these results reveal a high propensity of evodiamine to inhibit proliferation and metastasis of CCA in vivo without apparent toxicity-related events or significant body weight changes.

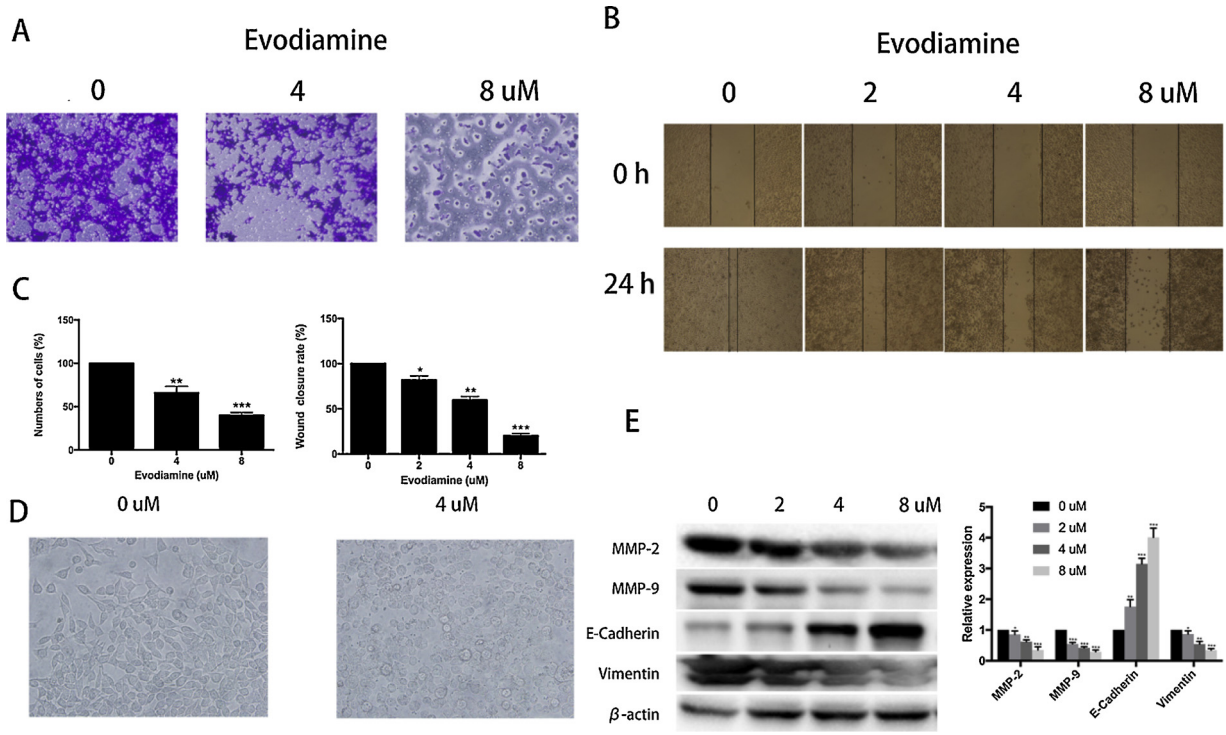

Fig. 3. Evodiamine suppresses CCA cell migration and invasion.
The effects of evodiamine on the migration and invasion of CCA cancer cells was explored. (A) Micrographs represent cell migration onto the underside of a transwell membrane under 100× magnification. (B) Micrographs represent cell migration under 40× magnification, before and after injury. (C) The cell number of each field was counted and averaged. Migrated cells were expressed relative to the control group. (D) Phase contrast microscopy. All images were obtained at a magnification of × 100. (E)The effects of evodiamine on relative protein expression. The data are expressed as the mean SD of 3 replicate experiments. Significant differences from the control are indicated by $*P < 0.05$, $**P < 0.01$, $***P < 0.001$.

4. Discussion

CCA is the second most common hepatobiliary malignancy and has emerged as one of the leading causes of cancer-related deaths worldwide (Rizvi et al., 2017). More effective therapeutic approaches are urgently needed to improve the outcomes of CCA treatment. Evodiamine has been used as a traditional Chinese medicine for many years (Jiang et al., 2017). Previous studies have reported that evodiamine reduces the phosphorylation of STAT3 (Tyr705) in human colorectal cancer cells and in HCC (Yang et al., 2013; Zhao et al., 2015a). However, the effects of evodiamine on CCA and the role of STAT3 in evodiamine-mediated CCA inhibition have not yet been investigated. In the present study, we showed that evodiamine inhibits the cell growth and invasion through IL-6/ STAT3 signaling axis in CCA cells, and that SHP-2 is a key modulator of dephosphorylation of IL-6/STAT3. Inhibition of SHP-2 expression reversed the aforementioned effects of evodiamine. In a xenograft tumor model, evodiamine elicited impressive anti-tumor actions to limit tumor growth and metastasis in a mouse xenograft model of CCA, as indicated by the significant decreases in tumor size in the evodiamine-treated animals. To our knowledge, this is the first study to demonstrate the anti-tumor effect of evodiamine and its underlying mechanism in CCA cancer cells.

Apoptosis, i.e., programmed cell death, plays a vital role in eliminating mutated or malignant cells (Bhola and Letai, 2016; Zhang et al., 2016). Various natural compounds are known to prevent the growth of tumor cells through inducing apoptosis (Dvorakova and Landa, 2017; Hu et al., 2017b). Previous studies have shown that evodiamine inhibits the growth of HCC cells and colorectal cancer cells by inducing apoptosis (Wang et al., 2008; Yang et al., 2013). Our data also demonstrate that CCA cells treated with evodiamine exhibit specific morphological changes consistent with apoptosis. In addition, flow cytometry data further indicated that the percentage of apoptotic CCA cells dramatically increased following treatment with evodiamine. Persistent STAT3 activation suppresses the expression levels of anti-apoptotic proteins and up-regulates the expression levels of pro-apoptotic proteins. Bax and Bcl-2 have been reported to be involved in the mitochondria-associated apoptosis pathway (Altieri, 2013; Moldoveanu et al., 2014). Increased levels of Bax and decreased levels of Bcl-2 can lead to a loss of mitochondrial membrane potential and trigger a series of apoptotic events, including the activation of caspase 9 and caspase 3. Cleaved caspase 9 further activates caspase 3, a key enzyme in the intrinsic apoptosis pathway, to induce subsequent apoptotic events (Kermer et al., 2000). In the present study, we found that evodiamine decreased the Bcl-2 level and increased the levels of Bax and cleaved caspase 3 and caspase 9. Therefore, evodiamine might induce apoptosis via the mitochondria-associated apoptosis pathway in CCA cells.

We also found that evodiamine effectively suppressed CCA cell migration and invasion. It is well known that the EMT is a major factor in the invasion and migration of cancer cells (Li and Li, 2015). The cell status of mesenchymal-like phenotype and epithelial-like phenotype can be transformed for each other when conditions change. When cells undergo the EMT, epithelial markers, such as E-cadherin, decrease, whereas mesenchymal markers, such as vimentin, MMP2 and MMP9, increase (Qin et al., 2012). We demonstrated that evodiamine significantly inhibited the migration and invasion of CCA cells and reduced the expression levels of MMP-2 and MMP-9 while increasing the E-cadherin protein expression in a dose-dependent manner. These findings indicate that evodiamine could suppress CCA migration and invasion via reversing CCA cells EMT.

Different mechanisms underlying the anti-tumor effects of evodiamine have been reported in different types of tumor cells (Yang et al., 2018; Zhao et al., 2015b; Zhong et al., 2015). STAT3 activation is initiated by phosphorylation, followed by dimerization and translocation into the nucleus, where it regulates the transcription of target genes

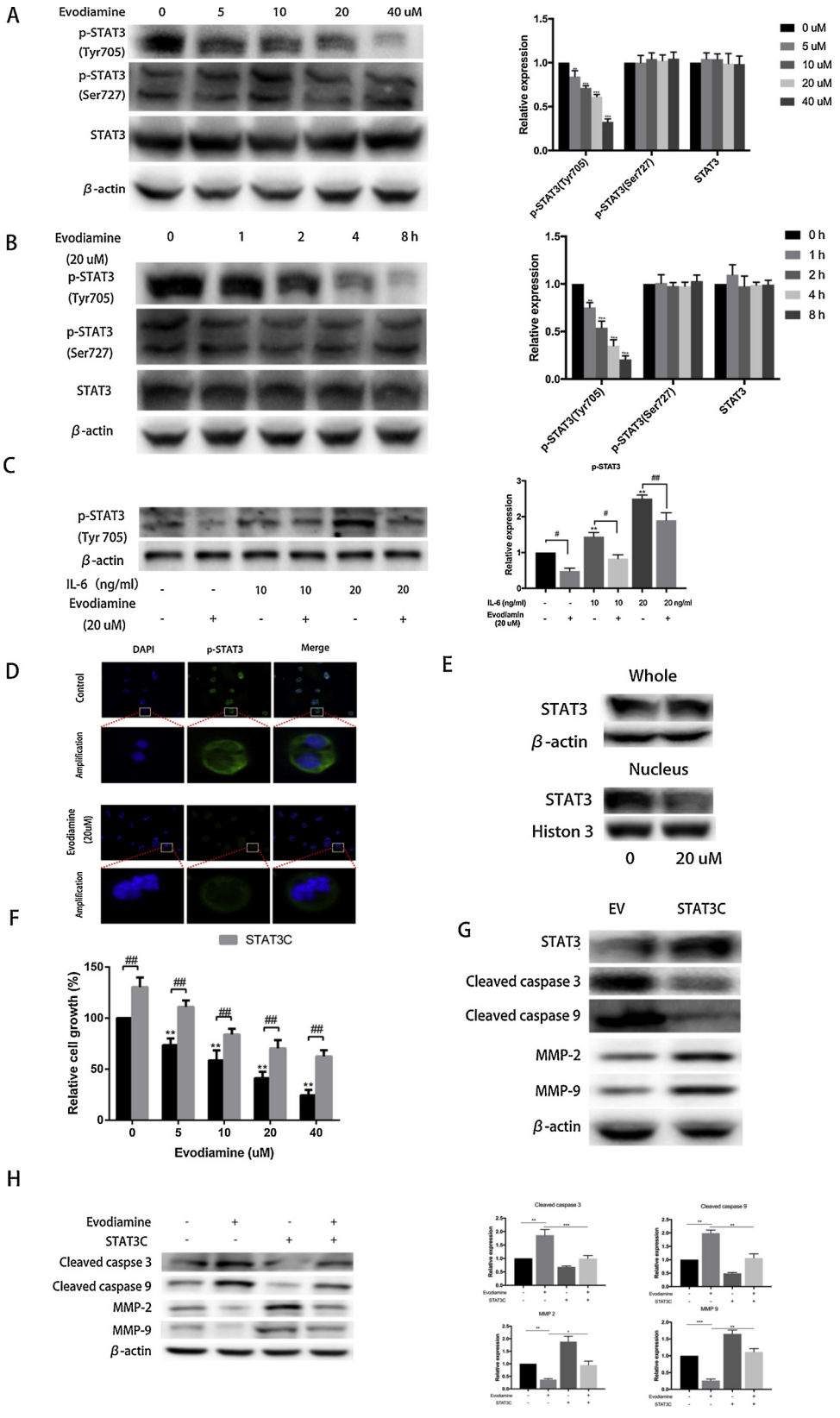

Fig. 4. The inhibitory effect of evodiamine on CCA cell proliferation is dependent on the suppression of persistent IL-6/STAT3 activation.

Inhibitory effects of evodiamine is dependent on the suppression of persistent STAT3 activation. (A & B) TFK-1 cells were treated with evodiamine for the indicated concentrations and indicated time, followed by western blot. (C) TFK-1 cells were pretreated with evodiamine (20 μM) for 24 h and then stimulated with indicated concentrations of IL-6 (0, 10 or 20 ng/ml) for 15 min, followed by Western blot. (D) Representative fluorescence microscope images revealed the nucleus levels of STAT3 (red). (E) The expression levels of STAT3 in whole-cell lysates and nucleus were analyzed by western blot. (F) TFK-1 cells were transfected with empty vector or STAT3C plasmid for 24 h and then treated with evodiamine at the indicated concentrations for 24 h. Cell viability was measured by CCK8 assay. (G) Cell lysates from EV or STAT3C-transfected TFK-1 cells were analyzed by western blot. (H) TFK-1 cells were transfected with STAT3C or empty vector (EV) for 48 h followed by evodiamine treatment for 24 h. Relative protein levels were measured by Western blot. The data are expressed as the mean SD of 3 replicate experiments. Significant differences from the control are indicated by $*P < 0.05$, $**P < 0.01$, $***P < 0.001$, $\#P < 0.05$ and $\#\#P < 0.01$.

(Vogt and Hart, 2011), participating in oncogenesis, such as apoptosis inhibitors (Bcl-2, and Survivin), cell-cycle regulators (cyclin D1) and EMT regulators (MMPs, vimentin) (Burdon et al., 2002; Qin et al., 2012; Xiang et al., 2016). IL-6 is often expressed when there are stimuli that are associated with cell damage or the expression of other pro-inflammatory cytokines (Banerjee and Resat, 2016). It can be overexpressed during inflammation and then lead to the activation of JAK proteins, which are responsible for intracellular signalling and the subsequent phosphorylation of STAT transcription factors, in particular STAT3 (Johnstone et al., 2015). In addition, A few studies demonstrated that IL-6 is partly produced by CCA cells acts by an autocrine mechanism (Wehbe et al., 2006). The IL-6/STAT3 signaling plays an

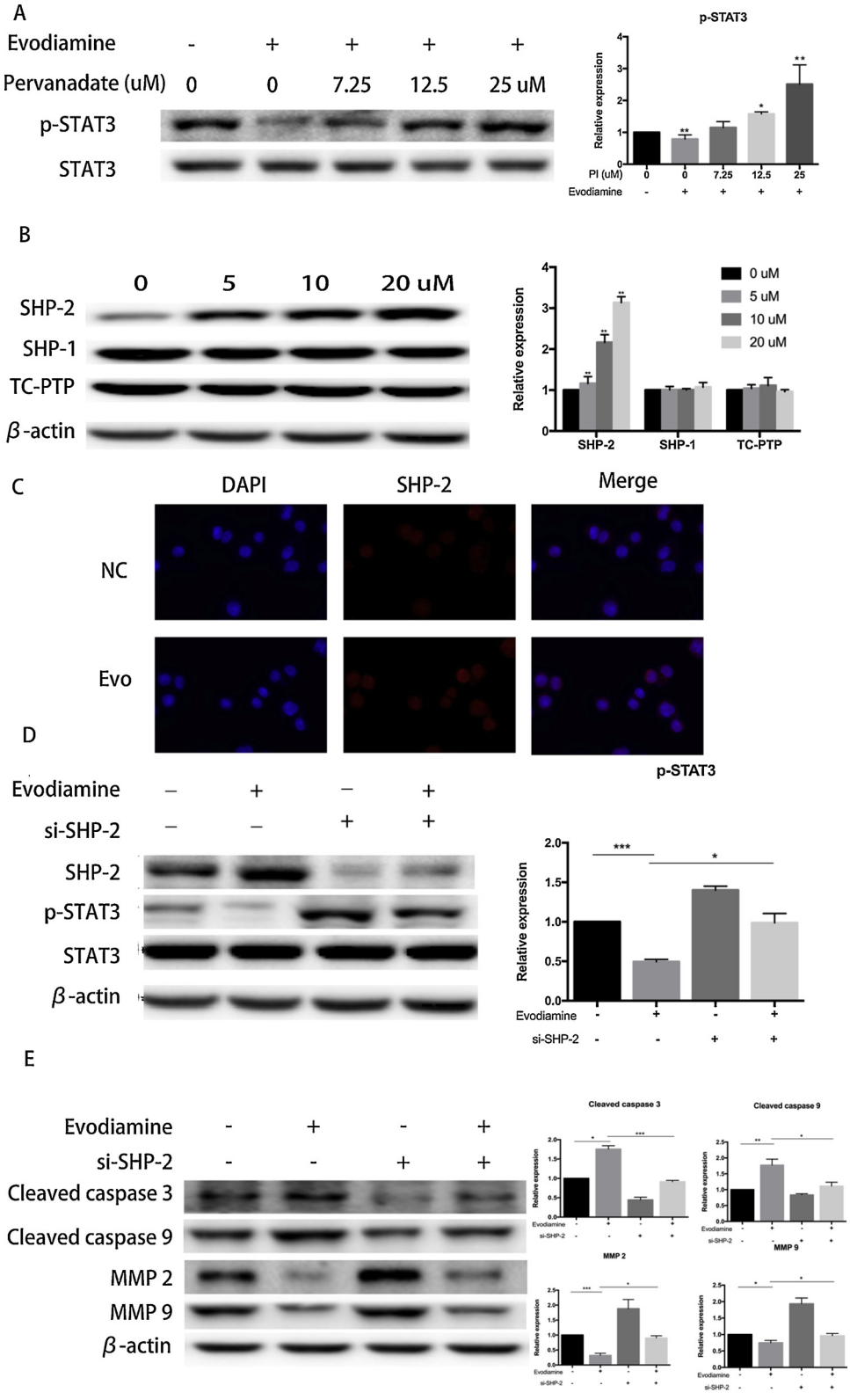

Fig. 5. Inhibitory effect of evodiamine on p-STAT3 is mediated by SHP-2.
Inhibitory effect of evodiamine on p-STAT3 is mediated by SHP-2. (A) Sodium pervanadate reverses the inhibitory effect of evodiamine on STAT3 activation. TFK-1 were treated with sodium pervanadate at indicated concentration for 1 h, and with additional 20 μM evodiamine for 2 h. Proteins were analyzed by western blotting with STAT3, p-STAT3 Tyr705. (B) TFK-1 cells were treated with indicated concentrations of evodiamine for 24 h. Proteins were analyzed by western blot with SHP-1, TC-PTP, SHP-2 and β-actin antibodies. (C) Representative fluorescence microscope images revealed the levels of SHP-2 (red). Nucleus were stained with DAPI (blue). (D) TFK-1 cells were transfected with si-SHP-2 or negative control (NC) for 48 h followed by evodiamine treatment for 2 h, and western blot analysis was performed. (E) TFK-1 cells were transfected with si-SHP-2 or negative control (NC) for 48 h followed by evodiamine treatment for 24 h, and western blot analysis was performed. (*P < 0.05; **P < 0.01; ***P < 0.001).

important role in various human cancers including CCA (Lin et al., 2016; Zheng et al., 2014; Zhou et al., 2015). It has been recognized that STAT3 inhibitors have tumor suppressive effects on various tumors. AG490, an important STAT3 inhibitor, can induce CCA cell apoptosis and then subsequently inhibits CCA cell proliferation (Lis et al., 2017; Liu et al., 2017a). Fuzheng Kang-Ai, a Chinese Herbal Medicine, induces Lung Cancer Cell Apoptosis via STAT3 Pathway. LKB1 inhibits the progression of gallbladder carcinoma via the suppression of STAT3 pathway (Wang et al., 2018). It is therefore conceivable that STAT3 is a potential therapeutic target for CCA treatment. Considering evodiamine has been shown to exhibit a strong inhibitory effect on different types of cancers. Present studies were performed to find whether the inhibitory effects of evodiamine was STAT3 phosphorylation (Tyr705) inhibition in CCA cells. Interestingly, evodiamine-induced inhibition of tyrosine

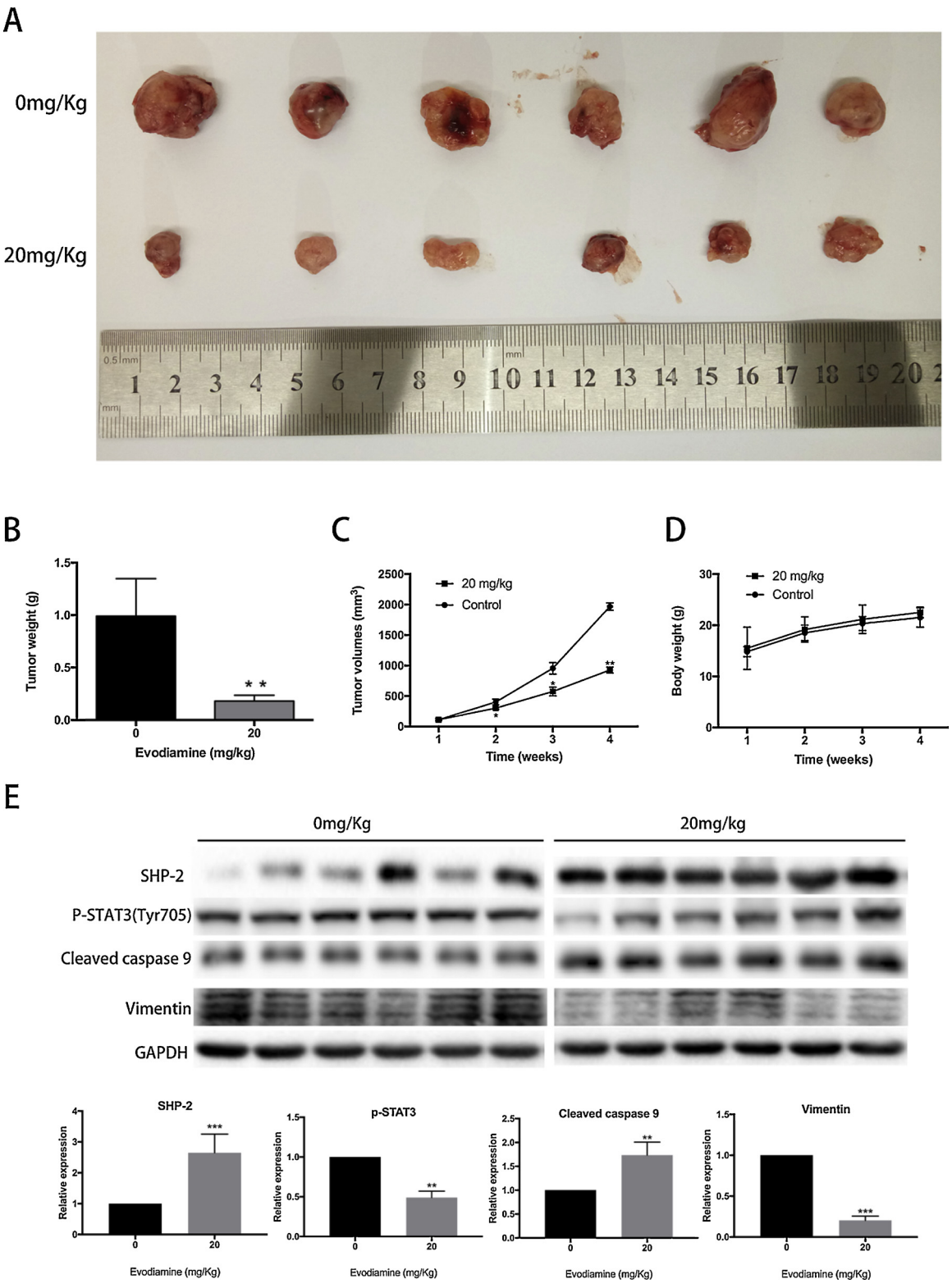

Fig. 6. Evodiamine inhibits tumor growth *in vivo* in xenograft tumor-bearing nude mice.
Effects of Evodiamine on xenograft tumor model (A) Photos of 6 representative tumors excised from the animals of each group are presented to show the sizes of the resulting tumors. (B) Statistical analysis of tumor weight. (C) Statistical analysis of tumor volume. (D) Statistical analysis of body weight. (E) Protein expression was analyzed by western blot. The data are expressed as the mean SD of 3 replicate experiments. Significant differences from the control are indicated by $^{*}P < 0.05$, $^{**}P < 0.01$, $^{***}P < 0.001$.

phosphorylation was observed for STAT3. STAT3 has two phosphorylation sites, Tyr705 and Ser727. The Tyr705 site is the main phosphorylation site of STAT3, and Ser727 phosphorylation is considered a secondary event after Tyr705 phosphorylation (Sakaguchi et al., 2012). In our present study, we found that the inhibitory effect of evodiamine was due to the phosphorylation at Tyr705 site but not Ser727-

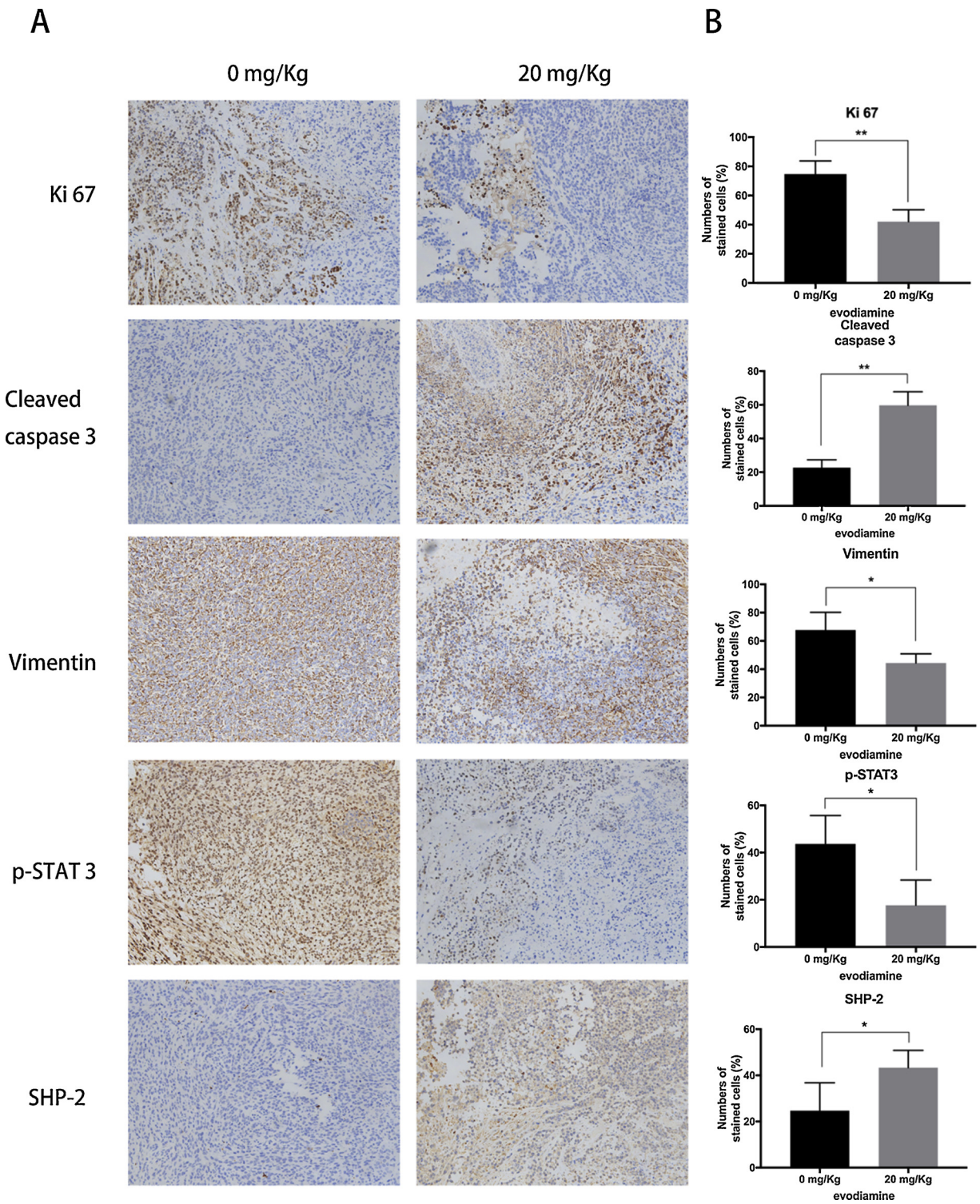

Fig. 7. Immunohistochemical characterization of evodiamine treatment mice.
(A) Tumor tissues were examined by IHC staining with antibodies against Ki67, cleaved caspase 3, Vimentin, p-STAT3 and SHP-2. The data are expressed as the mean SD of 3 replicate experiments. (B) The levels of stained cells were quantified. Data are expressed as mean ± S.E.M., n = 5 for each group. Significant differences from the control are indicated by $*P < 0.05$, $**P < 0.01$, $***P < 0.001$.

phosphorylated site. These results suggest that evodiamine specifically inhibited phosphorylation of STAT3 at Tyr705 site (Mai et al., 2018).

Several PTPs (eg., SHP-1 (Han et al., 2006), SHP-2 (Yang et al., 2011), TC-PTP (Lee et al., 2017)) were involved in negatively regulating IL-6/STAT3 pathway signaling. In CCA, the role of PTPs for inhibition of STAT3 have been rarely reported. Hu et al. showed that SC-43 activated PTP activity, leading to p-STAT3 and downstream cyclin B1 and Cdc2 downregulation, which induced G2-M arrest and apoptotic cell death in CCA cells (Hu et al., 2017c). Thus, PTPs may be a promising phosphatase for inactivation of STAT3 signaling in CCA cancer cells. Our further studies found that evodiamine up-regulated SHP-2 expression, and suppression of SHP-2 by siRNA abrogated the inhibitory effect of evodiamine on p-STAT3 (Tyr705) activation in CCA cells. Evodiamine also up-regulated SHP-2 expression in TFK-1 cell

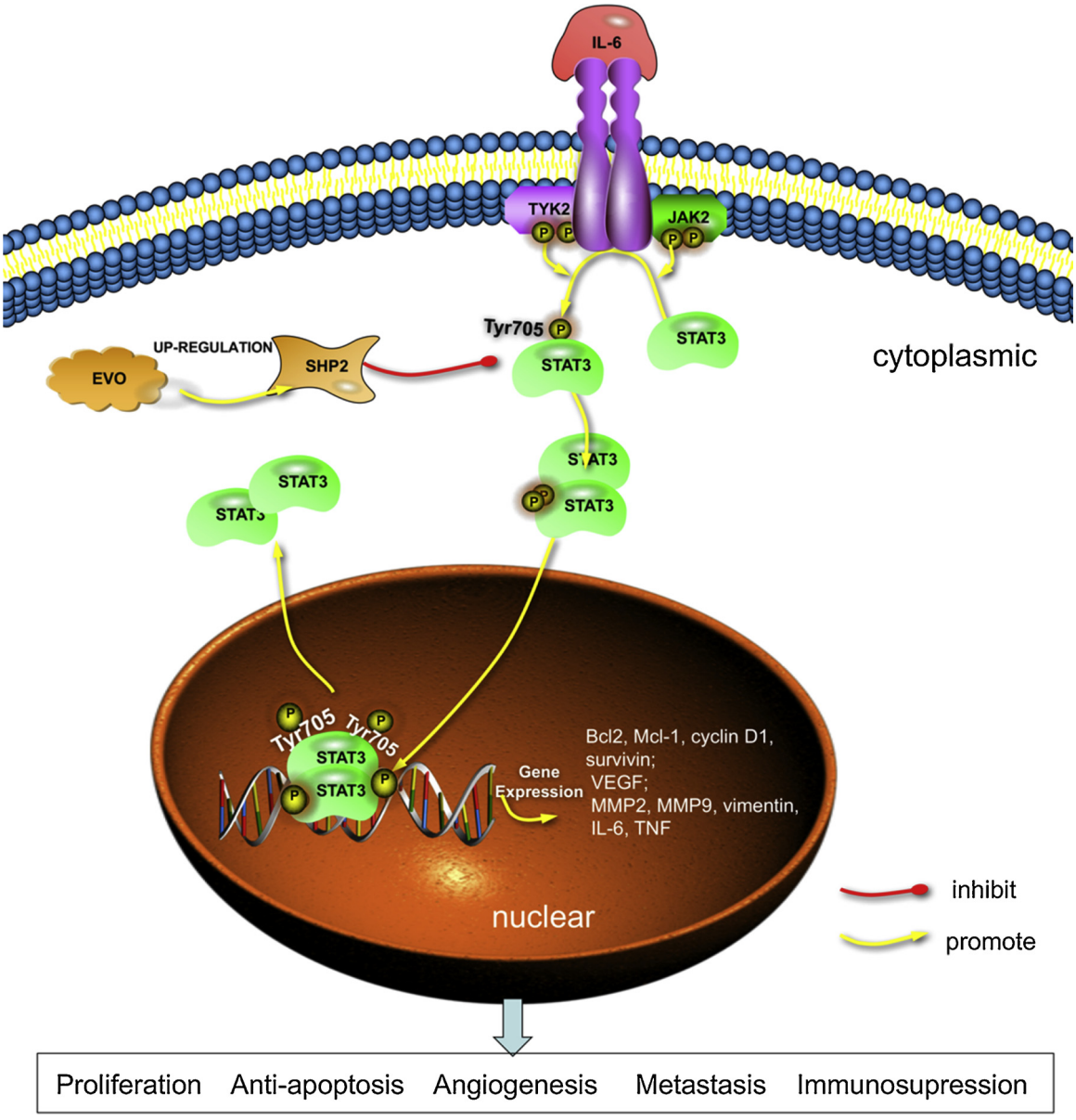

Fig. 8. A schematic summary for the inhibition mechanisms of evodiamine on STAT3 signaling pathway in the present study.

xenograft tumor. Therefore, SHP-2 is likely the phosphatase responsible for evodiamine induced p-STAT3 (Tyr705) dephosphorylation. In addition, evodiamine had no effects on SHP-1 and TC-PTP. Whether evodiamine affect other phosphatases requires further investigation. In addition, SHP-2 knockout mice might a better option for conforming the results, and it would be used in our further studies.

Various evidence showed that evodiamine regulates cell gene expression except for our present study. Xiao-Long Yuan et al. showed that evodiamine inhibits cycle-related genes (e.g. p53, Cdc14, TGF-β, Smad2, GADD45, Chk1, Mcm5, and Mcm6) (Yuan et al., 2017). Yang et al. demonstrated that evodiamine regulates autophagy related genes (e.g. Beclin 1 and LC3) (Yang et al., 2008). Further studies needs to be performed to explore whether evodiamine have effects on CCA through these gene regulation. It has been reported that evodiamine also exhibited inhibitory effect on PI3K/Akt/ NF-κB activation in pancreatic cancer (Zhou and Wu, 2006). There may be relationship between the blockage of STAT3 (Tyr705) activation and PI3K/Akt/ NF-κB activation by evodiamine because several genes (e.g., cyclin D1, Bcl-2 and survivin) related to cell survival and proliferation and are regulated by STAT3 and PI3K/Akt/ NF-κB were down-regulated by evodiamine. However, which mechanism involved in this relationship between STAT3 pathway and PI3K/Akt/ NF-κB pathway remain to be further investigated.

The *in vivo* study revealed a significant reduction in relative tumor size and volume in the evodiamine-treated animals. In addition, evodiamine exhibited low toxicity, and animal weight did not change significantly over the course of the experiment. Increased protein levels of cleaved caspase 9 was accompanied by decreased vimentin and p-STAT3 (Tyr705) expression in the evodiamine-treated animals. These results are consistent with the *in vitro* data.

5. Conclusion

In summary, our study found that evodiamine blocked STAT3 signaling pathway for the first time and this blockage was mediated by induction of SHP-2. (Fig. 8) The inhibition of STAT3 (Tyr705) phosphorylation triggered down-regulation of gene products related to cell apoptosis and cell EMT. And more importantly, evodiamine exhibited anti-tumor effect in TFK-1 xenograft nude mice model. These results suggested that evodiamine is a potential candidate to treat CCA.

Conflict of interest

Author Bi-Qiang Zhu declares that he has no conflict of interest. Author Lei Zhao declares that he has no conflict of interest. Author Yang Liu declares that he has no conflict of interest. Author Ye Jin declares that he has no conflict of interest. Author Jing Feng declares that he has no conflict of interest. Author Fu-Ya Zhao declares that he has no conflict of interest. Author Jia-Yu Sun declares that he has no conflict of interest. Author Rui Geng declares that he has no conflict of interest.

Funding

The work was supported by the Heilongjiang provincial academy of medical sciences [CR201415], the First Affiliated Hospital of Harbin Medical University [2012LX001] and the Harbin Science and Technology Bureau [2012RFLXS034].

Ethical approval

All animal studies were performed in accordance with the International Association for Assessment and Accreditation of Laboratory Animal Care institutional guidelines.

This article does not contain any studies with human participants performed by any of the authors.

Acknowledgements

We thank the assistance of the Translational Medicine Research and Cooperation Center of Northern China, where the experiments were performed.

References

Altieri, D.C., 2013. Targeting survivin in cancer. Cancer Lett. 332 (2), 225–228.
Banerjee, K., Resat, H., 2016. Constitutive activation of STAT3 in breast cancer cells: a review. Int. J. Cancer 138 (11), 2570–2578.
Bartolowits, M.D., Brown, W., Ali, R., Pedley, A.M., Chen, Q., Harvey, K.E., Wendt, M.K., Davisson, V.J., 2017. Selective inhibition of STAT3 phosphorylation using a nuclear-targeted kinase inhibitor. ACS Chem. Biol. 12 (9), 2371–2378.
Bhola, P.D., Letai, A., 2016. Mitochondria-judges and executioners of cell death sentences. Mol. Cell 61 (5), 695–704.
Burdon, T., Smith, A., Savatier, P., 2002. Signalling, cell cycle and pluripotency in embryonic stem cells. Trends Cell Biol. 12 (9), 432–438.
Chin, Y.T., Wang, L.M., Hsieh, M.T., Shih, Y.J., Nana, A.W., Changou, C.A., Yang, Y.S.H., Chiu, H.C., Fu, E., Davis, P.J., Tang, H.Y., Lin, H.Y., 2017. Leptin OB3 peptide suppresses leptin-induced signaling and progression in ovarian cancer cells. J. Biomed. Sci. 24 (1), 51.
Dvorakova, M., Landa, P., 2017. Anti-inflammatory activity of natural stilbenoids: a review. Pharmacol. Res. 124, 126–145.
Fang, C., Zhang, J., Qi, D., Fan, X., Luo, J., Liu, L., Tan, Q., 2014. Evodiamine induces G2/M arrest and apoptosis via mitochondrial and endoplasmic reticulum pathways in H446 and H1688 human small-cell lung cancer cells. PLoS One 9 (12), e115204.
Galluzzi, L., Lopez-Soto, A., Kumar, S., Kroemer, G., 2016. Caspases connect cell-death signaling to organismal homeostasis. Immunity 44 (2), 221–231.
Han, Y., Amin, H.M., Franko, B., Frantz, C., Shi, X., Lai, R., 2006. Loss of SHP1 enhances JAK3/STAT3 signaling and decreases proteosome degradation of JAK3 and NPM-ALK in ALK+ anaplastic large-cell lymphoma. Blood 108 (8), 2796–2803.
Hu, C.Y., Wu, H.T., Su, Y.C., Lin, C.H., Chang, C.J., Wu, C.L., 2017a. Evodiamine exerts an anti-hepatocellular carcinoma activity through a WWOX-Dependent pathway. Molecules 22 (7).
Hu, K., Miao, L., Goodwin, T.J., Li, J., Liu, Q., Huang, L., 2017b. Quercetin remodels the tumor microenvironment to improve the permeation, retention, and antitumor effects of nanoparticles. ACS Nano 11 (5), 4916–4925.
Hu, M.H., Chen, L.J., Chen, Y.L., Tsai, M.S., Shiau, C.W., Chao, T.I., Liu, C.Y., Kao, J.H., Chen, K.F., 2017c. Targeting SHP-1-STAT3 signaling: a promising therapeutic approach for the treatment of cholangiocarcinoma. Oncotarget 8 (39), 65077–65089.
Jiang, X.H., Wu, Q.Q., Xiao, Y., Yuan, Y., Yang, Z., Bian, Z.Y., Chang, W., Tang, Q.Z., 2017. Evodiamine prevents isoproterenol-induced cardiac fibrosis by regulating endothelial-to-Mesenchymal transition. Planta Med. 83 (9), 761–769.
Jin, Y., Yoon, Y.J., Jeon, Y.J., Choi, J., Lee, Y.J., Lee, J., Choi, S., Nash, O., Han, D.C., Kwon, B.M., 2017. Geranylnaringenin (CG902) inhibits constitutive and inducible STAT3 activation through the activation of SHP-2 tyrosine phosphatase. Biochem. Pharmacol. 142, 46–57.
Johnstone, C.N., Chand, A., Putoczki, T.L., Ernst, M., 2015. Emerging roles for IL-11 signaling in cancer development and progression: focus on breast cancer. Cytok. Growth Factor Rev. 26 (5), 489–498.
Kan, S.F., Yu, C.H., Pu, H.F., Hsu, J.M., Chen, M.J., Wang, P.S., 2007. Anti-proliferative effects of evodiamine on human prostate cancer cell lines DU145 and PC3. J. Cell. Biochem. 101 (1), 44–56.
Kermer, P., Ankerhold, R., Klocker, N., Krajewski, S., Reed, J.C., Bahr, M., 2000. Caspase-9: involvement in secondary death of axotomized rat retinal ganglion cells in vivo. Brain Res. Mol. Brain Res. 85 (1-2), 144–150.
Khuntikeo, N., Pugkhem, A., Titapun, A., Bhudhisawasdi, V., 2014. Surgical management of perihilar cholangiocarcinoma: a Khon Kaen experience. J. Hepatobiliary Pancreat. Sci. 21 (8), 521–524.
Lee, H., Kim, M., Baek, M., Morales, L.D., Jang, I.S., Slaga, T.J., DiGiovanni, J., Kim, D.J., 2017. Targeted disruption of TC-PTP in the proliferative compartment augments STAT3 and AKT signaling and skin tumor development. Sci. Rep. 7, 45077.
Li, L., Li, W., 2015. Epithelial-mesenchymal transition in human cancer: comprehensive reprogramming of metabolism, epigenetics, and differentiation. Pharmacol. Ther. 150, 33–46.
Lin, K.Y., Ye, H., Han, B.W., Wang, W.T., Wei, P.P., He, B., Li, X.J., Chen, Y.Q., 2016. Genome-wide screen identified let-7c/miR-99a/miR-125b regulating tumor progression and stem-like properties in cholangiocarcinoma. Oncogene 35 (26), 3376–3386.
Lis, C., Rubner, S., Roatsch, M., Berg, A., Gilcrest, T., Fu, D., Nguyen, E., Schmidt, A.M., Krautscheid, H., Meiler, J., Berg, T., 2017. Development of Erasin: a chromone-based STAT3 inhibitor which induces apoptosis in Erlotinib-resistant lung cancer cells. Sci. Rep. 7 (1), 17390.
Liu, J.F., Deng, W.W., Chen, L., Li, Y.C., Wu, L., Ma, S.R., Zhang, W.F., Bu, L.L., Sun, Z.J., 2017a. Inhibition of JAK2/STAT3 reduces tumor-induced angiogenesis and myeloid-derived suppressor cells in head and neck cancer. Mol. Carcinog.
Liu, X., Su, X., Xu, S., Wang, H., Han, D., Li, J., Huang, M., Cao, X., 2017b. MicroRNA in vivo precipitation identifies miR-151-3p as a computational unpredictable miRNA to target Stat3 and inhibits innate IL-6 production. Cell. Mol. Immunol.
Ma, D.L., Liu, L.J., Leung, K.H., Chen, Y.T., Zhong, H.J., Chan, D.S., Wang, H.M., Leung, C.H., 2014. Antagonizing STAT3 dimerization with a rhodium(III) complex. Angew. Chem. Int. Ed. Engl. 53 (35), 9178–9182.
Mai, T., Markov, G.J., Brady, J.J., Palla, A., Zeng, H., Sebastiano, V., Blau, H.M., 2018. NKX3-1 is required for induced pluripotent stem cell reprogramming and can replace OCT4 in mouse and human iPSC induction. Nat. Cell Biol. 20 (8), 900–908.
Moldoveanu, T., Follis, A.V., Kriwacki, R.W., Green, D.R., 2014. Many players in BCL-2 family affairs. Trends Biochem. Sci. 39 (3), 101–111.
Mott, J.L., Gores, G.J., 2007. Targeting IL-6 in cholangiocarcinoma therapy. Am. J. Gastroenterol. 102 (10), 2171–2172.
Qin, Q., Xu, Y., He, T., Qin, C., Xu, J., 2012. Normal and disease-related biological functions of Twist1 and underlying molecular mechanisms. Cell Res. 22 (1), 90–106.
Razumilava, N., Gores, G.J., Lindor, K.D., 2011. Cancer surveillance in patients with primary sclerosing cholangitis. Hepatology 54 (5), 1842–1852.
Reyna, D.E., Garner, T.P., Lopez, A., Kopp, F., Choudhary, G.S., Sridharan, A., Narayanagari, S.R., Mitchell, K., Dong, B., Bartholdy, B.A., Walensky, L.D., Verma, A., Steidl, U., Gavathiotis, E., 2017. Direct activation of BAX by BTSA1 overcomes apoptosis resistance in acute myeloid leukemia. Cancer Cell 32 (4), 490–505 e410.
Rizvi, S., Gores, G.J., 2017. Emerging molecular therapeutic targets for cholangiocarcinoma. J. Hepatol. 67 (3), 632–644.
Rizvi, S., Borad, M.J., Patel, T., Gores, G.J., 2014. Cholangiocarcinoma: molecular pathways and therapeutic opportunities. Semin. Liver Dis. 34 (4), 456–464.
Rizvi, S., Khan, S.A., Hallemeier, C.L., Kelley, R.K., Gores, G.J., 2017. Cholangiocarcinoma - evolving concepts and therapeutic strategies. Nat. Rev. Clin. Oncol.
Rokavec, M., Oner, M.G., Li, H., Jackstadt, R., Jiang, L., Lodygin, D., Kaller, M., Horst, D., Ziegler, P.K., Schwitalla, S., Slotta-Huspenina, J., Bader, F.G., Greten, F.R., Hermeking, H., 2014. IL-6R/STAT3/miR-34a feedback loop promotes EMT-mediated colorectal cancer invasion and metastasis. J. Clin. Invest. 124 (4), 1853–1867.
Roy, R., Dagher, A., Butterfield, C., Moses, M.A., 2017. ADAM12 is a novel regulator of tumor angiogenesis via STAT3 signaling. Mol. Cancer Res.
Sakaguchi, M., Oka, M., Iwasaki, T., Fukami, Y., Nishigori, C., 2012. Role and regulation of STAT3 phosphorylation at Ser727 in melanocytes and melanoma cells. J. Invest. Dermatol. 132 (7), 1877–1885.
Shi, C.S., Li, J.M., Chin, C.C., Kuo, Y.H., Lee, Y.R., Huang, Y.C., 2017a. Evodiamine induces cell growth arrest, apoptosis and suppresses tumorigenesis in human urothelial cell carcinoma cells. Anticancer Res. 37 (3), 1149–1159.
Shi, J., Feng, J., Xie, J., Mei, Z., Shi, T., Wang, S., Du, Y., Yang, G., Wu, Y., Cheng, X., Li, S., Zhu, L., Yang, C.S., Tu, S., Jie, Z., 2017b. Targeted blockade of TGF-beta and IL-6/JAK2/STAT3 pathways inhibits lung cancer growth promoted by bone marrow-derived myofibroblasts. Sci. Rep. 7 (1), 8660.
Siddiquee, K., Zhang, S., Guida, W.C., Blaskovich, M.A., Greedy, B., Lawrence, H.R., Yip, M.L., Jove, R., McLaughlin, M.M., Lawrence, N.J., Sebti, S.M., Turkson, J., 2007. Selective chemical probe inhibitor of Stat3, identified through structure-based virtual screening, induces antitumor activity. Proc. Natl. Acad. Sci. U. S. A. 104 (18), 7391–7396.
Tanjak, P., Thiantanawat, A., Watcharasit, P., Satayavivad, J., 2018. Genistein reduces the activation of AKT and EGFR, and the production of IL6 in cholangiocarcinoma cells involving estrogen and estrogen receptors. Int. J. Oncol. 53 (1), 177–188.
Thiery, J.P., Acloque, H., Huang, R.Y., Nieto, M.A., 2009. Epithelial-mesenchymal transitions in development and disease. Cell 139 (5), 871–890.
Tong, M., Wang, J., Jiang, N., Pan, H., Li, D., 2017. Correlation between p-STAT3 overexpression and prognosis in lung cancer: a systematic review and meta-analysis. PLoS One 12 (8), e0182282.
Torzilli, P.A., Bourne, J.W., Cigler, T., Vincent, C.T., 2012. A new paradigm for

mechanobiological mechanisms in tumor metastasis. Semin. Cancer Biol. 22 (5-6), 385–395.
Vogt, P.K., Hart, J.R., 2011. PI3K and STAT3: a new alliance. Cancer Discov. 1 (6), 481–486.
Wang, X.N., Han, X., Xu, L.N., Yin, L.H., Xu, Y.W., Qi, Y., Peng, J.Y., 2008. Enhancement of apoptosis of human hepatocellular carcinoma SMMC-7721 cells through synergy of berberine and evodiamine. Phytomedicine 15 (12), 1062–1068.
Wang, T., Kusudo, T., Takeuchi, T., Yamashita, Y., Kontani, Y., Okamatsu, Y., Saito, M., Mori, N., Yamashita, H., 2013. Evodiamine inhibits insulin-stimulated mTOR-S6K activation and IRS1 serine phosphorylation in adipocytes and improves glucose tolerance in obese/diabetic mice. PLoS One 8 (12), e83264.
Wang, S., Wang, L., Shi, Z., Zhong, Z., Chen, M., Wang, Y., 2014. Evodiamine synergizes with doxorubicin in the treatment of chemoresistant human breast cancer without inhibiting P-glycoprotein. PLoS One 9 (5), e97512.
Wang, S., Long, S., Xiao, S., Wu, W., Hann, S.S., 2018. Decoction of chinese herbal medicine fuzheng kang-ai induces lung Cancer cell apoptosis via STAT3/Bcl-2/Caspase-3 pathway. Evid. Complem. Altern. Med. 2018, 8567905.
Wehbe, H., Henson, R., Meng, F., Mize-Berge, J., Patel, T., 2006. Interleukin-6 contributes to growth in cholangiocarcinoma cells by aberrant promoter methylation and gene expression. Cancer Res. 66 (21), 10517–10524.
Weissenberger, J., Priester, M., Bernreuther, C., Rakel, S., Glatzel, M., Seifert, V., Kogel, D., 2010. Dietary curcumin attenuates glioma growth in a syngeneic mouse model by inhibition of the JAK1,2/STAT3 signaling pathway. Clin. Cancer Res. 16 (23), 5781–5795.
Wu, Q.Q., Xiao, Y., Jiang, X.H., Yuan, Y., Yang, Z., Chang, W., Bian, Z.Y., Tang, Q.Z., 2017a. Evodiamine attenuates TGF-beta1-induced fibroblast activation and endothelial to mesenchymal transition. Mol. Cell. Biochem. 430 (1-2), 81–90.
Wu, W.S., Chien, C.C., Liu, K.H., Chen, Y.C., Chiu, W.T., 2017b. Evodiamine prevents glioma growth, induces glioblastoma cell apoptosis and cell cycle arrest through JNK activation. Am. J. Chin. Med. 45 (4), 879–899.
Xiang, S., Zhang, Q., Tang, Q., Zheng, F., Wu, J., Yang, L., Hann, S.S., 2016. Activation of AMPKalpha mediates additive effects of solamargine and metformin on suppressing MUC1 expression in castration-resistant prostate cancer cells. Sci. Rep. 6, 36721.
Xin, H., Herrmann, A., Reckamp, K., Zhang, W., Pal, S., Hedvat, M., Zhang, C., Liang, W., Scuto, A., Weng, S., Morosini, D., Cao, Z.A., Zinda, M., Figlin, R., Huszar, D., Jove, R., Yu, H., 2011. Antiangiogenic and antimetastatic activity of JAK inhibitor AZD1480. Cancer Res. 71 (21), 6601–6610.
Yang, J., Wu, L.J., Tashino, S., Onodera, S., Ikejima, T., 2008. Reactive oxygen species and nitric oxide regulate mitochondria-dependent apoptosis and autophagy in evodiamine-treated human cervix carcinoma HeLa cells. Free Radic. Res. 42 (5), 492–504.
Yang, Y., Jiang, B., Huo, Y., Primo, L., Dahl, J.S., Benjamin, T.L., Luo, J., 2011. Shp2 suppresses PyMT-induced transformation in mouse fibroblasts by inhibiting Stat3 activity. Virology 409 (2), 204–210.
Yang, J., Cai, X., Lu, W., Hu, C., Xu, X., Yu, Q., Cao, P., 2013. Evodiamine inhibits STAT3 signaling by inducing phosphatase shatterproof 1 in hepatocellular carcinoma cells. Cancer Lett. 328 (2), 243–251.
Yang, D., Li, L., Qian, S., Liu, L., 2018. Evodiamine ameliorates liver fibrosis in rats via TGF-beta1/Smad signaling pathway. J. Nat. Med. 72 (1), 145–154.
Yao, C., Su, L., Shan, J., Zhu, C., Liu, L., Liu, C., Xu, Y., Yang, Z., Bian, X., Shao, J., Li, J., Lai, M., Shen, J., Qian, C., 2016. IGF/STAT3/NANOG/Slug signaling Axis Simultaneously controls epithelial-mesenchymal transition and stemness maintenance in colorectal Cancer. Stem Cells 34 (4), 820–831.
Yuan, X.L., Zhang, P., Liu, X.M., Du, Y.M., Hou, X.D., Cheng, S., Zhang, Z.F., 2017. Cytological assessments and transcriptome profiling demonstrate that evodiamine inhibits growth and induces apoptosis in a renal carcinoma cell line. Sci. Rep. 7 (1), 12572.
Zhang, A., He, W., Shi, H., Huang, X., Ji, G., 2016. Natural compound oblongifolin C inhibits autophagic flux, and induces apoptosis and mitochondrial dysfunction in human cholangiocarcinoma QBC939 cells. Mol. Med. Rep. 14 (4), 3179–3183.
Zhao, L.C., Li, J., Liao, K., Luo, N., Shi, Q.Q., Feng, Z.Q., Chen, D.L., 2015a. Evodiamine induces apoptosis and inhibits migration of HCT-116 human colorectal Cancer cells. Int. J. Mol. Sci. 16 (11), 27411–27421.
Zhao, Z., Gong, S., Wang, S., Ma, C., 2015b. Effect and mechanism of evodiamine against ethanol-induced gastric ulcer in mice by suppressing Rho/NF-small ka, CyrillicB pathway. Int. Immunopharmacol. 28 (1), 588–595.
Zheng, T., Hong, X., Wang, J., Pei, T., Liang, Y., Yin, D., Song, R., Song, X., Lu, Z., Qi, S., Liu, J., Sun, B., Xie, C., Pan, S., Li, Y., Luo, X., Li, S., Fang, X., Bhatta, N., Jiang, H., Liu, L., 2014. Gankyrin promotes tumor growth and metastasis through activation of IL-6/STAT3 signaling in human cholangiocarcinoma. Hepatology 59 (3), 935–946.
Zhimin, G., Noor, H., Jian-Bo, Z., Lin, W., Jha, R.K., 2013. Advances in diagnosis and treatment of hilar cholangiocarcinoma – a review. Med. Sci. Monit. 19, 648–656.
Zhong, Z.F., Tan, W., Wang, S.P., Qiang, W.A., Wang, Y.T., 2015. Anti-proliferative activity and cell cycle arrest induced by evodiamine on paclitaxel-sensitive and -resistant human ovarian cancer cells. Sci. Rep. 5, 16415.
Zhou, L.G., Wu, J.Y., 2006. Development and application of medicinal plant tissue cultures for production of drugs and herbal medicinals in China. Nat. Prod. Rep. 23 (5), 789–810.
Zhou, Q.X., Jiang, X.M., Wang, Z.D., Li, C.L., Cui, Y.F., 2015. Enhanced expression of suppresser of cytokine signaling 3 inhibits the IL-6-induced epithelial-to-mesenchymal transition and cholangiocarcinoma cell metastasis. Med. Oncol. 32 (4), 105.
Zhu, J., Sun, C., Wang, L., Xu, M., Zang, Y., Zhou, Y., Liu, X., Tao, W., Xue, B., Shan, Y., Yang, D., 2016. Targeting survivin using a combination of miR494 and survivin shRNA has synergistic effects on the suppression of prostate cancer growth. Mol. Med. Rep. 13 (2), 1602–1610.